RI 9154

Bureau of Mines Report of Investigations/1988

Stiffness Characteristics of Longwall Shields

By Thomas M. Barczak and David E. Schwemmer

UNITED STATES DEPARTMENT OF THE INTERIOR

Report of Investigations 9154

Stiffness Characteristics of Longwall Shields

By Thomas M. Barczak and David E. Schwemmer

UNITED STATES DEPARTMENT OF THE INTERIOR
Donald Paul Hodel, Secretary

BUREAU OF MINES
David S. Brown, Acting Director

Library of Congress Cataloging in Publication Data:

Barczak, Thomas M.
Stiffness characteristics of longwall shields.

(Report of investigations / United States Department of the Interior, Bureau of Mines ; 9154)

Bibliography.

Supt. of Docs. no.: I 28.27:9154.

1. Longwall mining. 2. Mine roof control. I. Schwemmer, David E. II. Title. III. Series: Report of investigations (United States. Bureau of Mines) ; 9154.

TN23.U43 [TN275] 622 s [622.'.28] 87-600360

CONTENTS

	Page
Abstract	1
Introduction	2
Elastic stiffness model	3
Support specimens	5
Test procedure--shield stiffness determinations	5
Test results--shield stiffness characteristics	6
Shield height	6
Vertical shield stiffness	7
Horizontal shield stiffness	8
Cross-axis shield stiffness	8
Setting pressure	9
Shield load predictions from shield stiffnesses	10
Conclusions	11
Appendix A.--Description of shield supports	12
Appendix B.--Description of mine roof simulator	13
Appendix C.--Nomenclature	14

ILLUSTRATIONS

1.	Analysis of mine roof supports	2
2.	Elastically deformable body	4
3.	Strata displacements and shield reactions	4
4.	Vertical shield displacement tests	5
5.	Horizontal shield displacement tests	5
6.	Displacement load profile	6
7.	Vertical and horizontal shield stiffness as a function of shield height	7
8.	Cross-axis shield stiffness as a function of shield height	7
9.	Vertical stiffness characteristics at midpoints of operating range	7
10.	Effect of setting pressure on vertical and horizontal shield stiffness	9
11.	Setting pressure effects on cross-axis stiffness coefficients	9
12.	Predicted shield displacements from leg orientations and leg pressure measurements	10
13.	Force predictions from shield stiffnesses	10
A-1.	Shield support	12
B-1.	Mine roof simulator	13

TABLES

1.	Comparison of shield specimens	5
2.	Summary of test parameters	6

UNIT OF MEASURE ABBREVIATIONS USED IN THIS REPORT

ft^2	square foot	lb	pound
in	inch	psi	pound per square inch
kip	1,000 lb	s	second
kip/in	kips per inch	st	short ton

STIFFNESS CHARACTERISTICS OF LONGWALL SHEILDS

By Thomas M. Barczak[1] and David E. Schwemmer[2]

ABSTRACT

The stiffness characteristics of longwall shields were investigated in this Bureau of Mines study. Since longwall strata activity is characterized by roof-to-floor and face-to-waste displacements, a model with two degrees of freedom was used to describe the load-displacement relationship of the shield structure. The model considers the support as an elastic body and relates horizontal and vertical resultant forces acting on the support to associated displacements as a function of the stiffness of the support structure. Stiffness coefficients under full canopy and base contact configurations were determined by controlled displacement loading of longwall shields in the Bureau's Mine Roof Simulator (MRS). Three two-legged longwall shields of different manufacture were investigated. The stiffness characteristics of these shields were evaluated relative to two parameters, namely, shield height and setting pressure. The test results indicate a reduction in shield stiffness for increasing height. Setting pressure was found to have less of an effect on shield stiffness, producing only a slight increase in stiffness as setting pressure increased. Similar trends were observed for all three shields, indicating a similarity in stiffness characteristics for shields of the same basic configuration.

[1]Research physicist, Pittsburgh Research Center, Bureau of Mines, Pittsburgh, PA.
[2]Structural engineer, Boeing Services International, Pittsburgh, PA.

INTRODUCTION

The approach used by the Bureau of Mines in analyzing mine roof supports (in this case, longwall shields) is shown in figure 1. As indicated, some of the objectives are to (1) develop an understanding of the interaction of the support with the strata so that supports can be more closely engineered to the geological conditions in which they are employed and (2) optimize support designs by examining the bending moment distribution and energy transfer throughout the support. The stiffness of the support structure and of its individual components are important properties for consideration.

Roof supports should be evaluated in the context of a system, the system being composed of the environment (roof and floor strata) and the support structure (longwall shield). The interaction between the roof support structure and the strata is dependent upon the stiffness of the support structure and the strata, among other factors. Stiffness is a measure of the ability of a material (structure) to resist deformation from applied loading, with a stiffer structure being more difficult to deform (requiring larger force) than a softer (less stiff) structure. Mathematically, stiffness is defined as the ratio of load to displacement. Hence, a stiffer roof support structure will react a larger load in response to a converging environment (roof or floor) than will a softer support structure for the same displacement. The required support resistance (support capacity) thus depends upon the stiffness of the support structure, assuming displacement loading of the strata. Ideally, the support stiffness should minimize support reactions while maintaining stability of the strata, unless conditions warrant high reactive support forces, for example, to induce caving. The stiffness of the support sturcture needs to be considered if supports are to be closely engineered to the behavior of the strata and geological conditions in which they are employed.

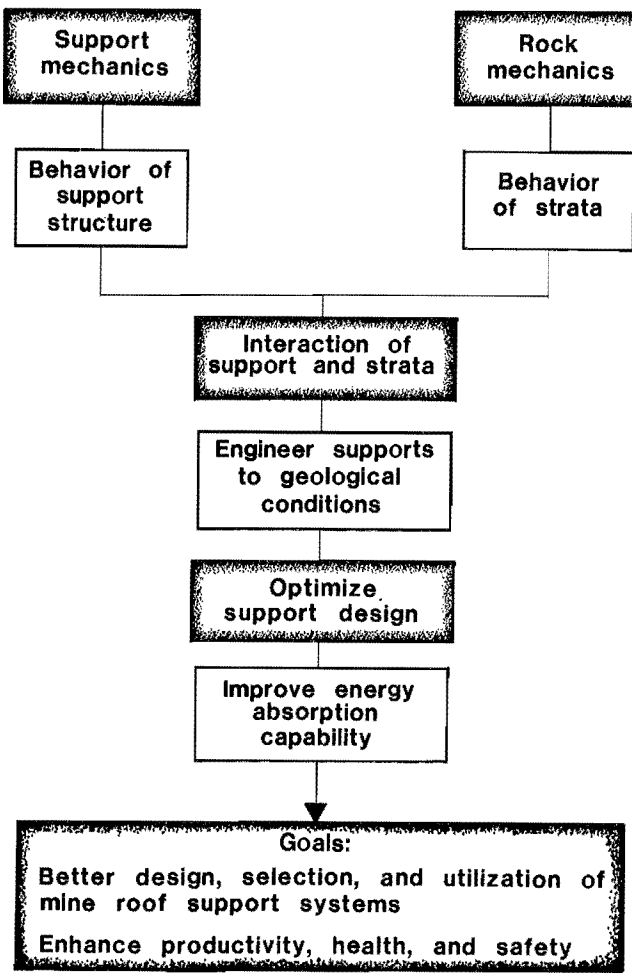

FIGURE 1.—Analysis of mine roof supports.

Describing the system from an energy approach, the force exerted by the strata as the roof or floor displacement occurs is equilibrated by the internal work (mostly strain energy) in the support structure. The distribution of this strain energy depends upon the load condition and relative stiffness of the support components. For the same displacement, stiffer components will assume more force than more flexible components. Since deformation can be produced from several types of loading or combinations of loading (i.e., axial, bending, shear, and torsion), it is difficult to make generalizations regarding the distribution of strain energy without examining the load condition and structural behavior and interaction of the components.

Three shield specimens, each of the same basic design, were evaluated. The study was limited to examination of the stiffness characteristics of the shield as a whole and parameters that affect overall shield stiffness, such as changes in shield height and setting pressure. The effect of contact conditions on shield stiffness was not evaluated. All loads were applied under full-contact canopy and base conditions. Under full contact load conditions, deformation of the canopy and base is minimal and is unlikely to have any significant effect on overall shield stiffness. The investigation of stiffness characteristics of specific components and resulting strain energy distribution is beyond the scope of this study and is being pursued in other studies. These studies are attempting to identify stress distribution and critical load conditions for shield supports.

Previous research in the use of shields as load monitors has generally been limited to rigid-body static analysis. Rigid-body analysis of shield mechanics (determining resultant forces acting on the shield canopy) requires elimination of unknowns (forces or moments) to produce a determinate solution compatible with static equilibrium requirements. Tests have shown that rigid-body analysis produces reasonably accurate determinations of resultant shield loading (horizontal and vertical forces acting on shield canopy).[3] However, one of the limitations of rigid-body analysis is that loads produced by vertical roof convergence cannot be distinguished from loads produced by horizontal (face-to-waste) strata activity.

Another limitation of rigid-body analysis is the inability to accurately determine stress (or bending moment) distribution within the support. Structures, including longwall shields, are never absolutely rigid; they deform under load. This deformation can significantly affect the resulting distribution of stresses (the strain energy distribution) in the shield components. Hence, an elastic analysis of shield mechanics is preferred.

The investigation of shield stiffness characteristics reported in this report is a first step in evaluating the load-deformation behavior of longwall shields and provides insight towards a more detailed elastic analyses and energy transfer investigation of shield supports. These efforts are primarily basic research into shield design and utilization. This investigation also has a practical application in that characterization of the shield stiffness enables the shield to be used as a monitor of strata loading and activity. More fundamentally, this investigation is intended to make mine operators more knowledgeable about the importance of shield stiffness in evaluating support reactions and strata control.

ELASTIC STIFFNESS MODEL

The concept of stiffness is illustrated in figure 2. If an elastic body is subjected to an external force, the body will be displaced (deformed) in proportion to the stiffness of the body.[4] Stiffness is a structural engineering term defined as the applied force required to produce a unit displacement in a structure (elastic body), expressed mathematically in the familiar Hooke's law form, where the resulting force is a linear function of the applied displacement:

[3]Barczak, T. M., and R. C. Garson. Technique to Measure Resultant Load Vector on Shield Supports. Pres. at 25th U.S. Symp. on Rock Mechanics in Productivity and Protection, Evanston, IL, June 25-27, 1984, pp. 667-680; available upon request from T. M. Barczak, BuMines, Pittsburgh, PA.

[4]Byars, E. F. Engineering Mechanics of Deformable Bodies. Intext Educ. Publ., 1975, pp. 88.

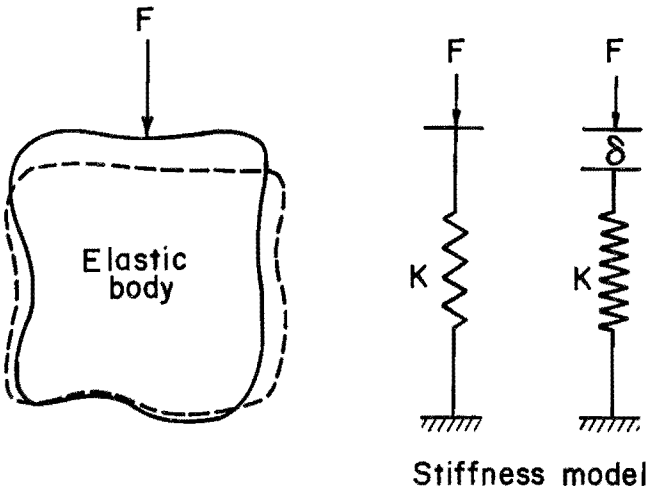

KEY

K Stiffness $\left(\frac{F}{\delta}\right)$

F Force

δ Displacement

FIGURE 2.—Elastically deformable body.

$$F = K \cdot \delta, \qquad (1)$$

where F = force (load),

δ = displacement,

and K = stiffness.

Therefore, if the stiffness of the body is known and the displacement measured, the resulting force can be determined.

This concept can be applied to shield roof supports if the support structure is assumed to act as an elastic body. Unlike the simple model presented in equation 1, where displacment was confined to one direction, the evaluation of longwall shields must consider displacements in two directions to account for both roof-to-floor (vertical) and face-to-waste (horizontal) strata convergence (fig. 3). Therefore, an elastic stiffness model with two degrees of freedom was examined:

$$F_v = K_1\delta_v + K_2\delta_h \qquad (2)$$

and

$$F_h = K_3\delta_v + K_4\delta_h, \qquad (3)$$

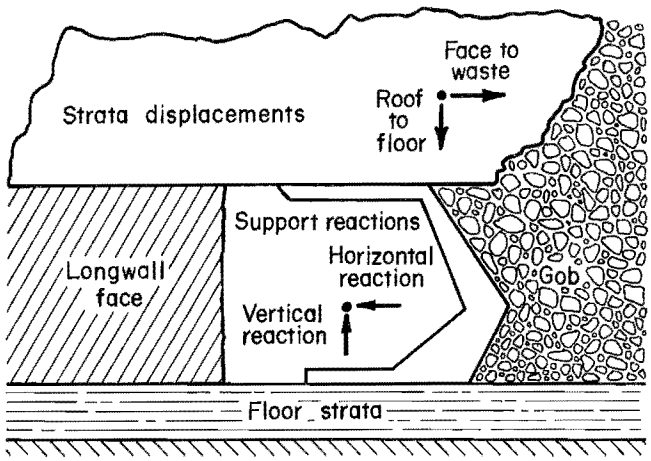

FIGURE 3.—Strata displacements and shield reactions.

where F_v = resultant vertical force,

F_h = resultant horizontal force,

δ_v = vertical displacement,

δ_h = horizontal displacement,

and K_1, K_2,

K_3, and K_4 = stiffness coefficients.

The kinematics of the shield support causes vertical roof convergence to produce not only a vertical support reaction, but also a horizontal roof support reaction (fig. 3). Likewise, horizontal strata displacement produces not only a horizontal support reaction, but also a vertical support reaction. This load-displacement behavior is reflected in the elastic stiffness model. Vertical shield stiffness (vertical force produced by vertical displacement) is represented by stiffness coefficient K_1, while K_4 represents horizontal shield stiffness (horizontal force produced by horizontal displacement). Terms K_2 and K_3 are referred to as cross-axis coefficients; they represent the ratios of vertical force produced by horizontal displacement and horizontal force produced by vertical displacement, respectively.

SUPPORT SPECIMENS

TABLE 1. - Comparison of shield specimens

Shield	Weight, st	Contact area, ft^2		Operating range, in	Capacity, st	Yield pressure, psi
		Canopy	Base			
1.....	14	43	19	60-130	360	6,100
2.....	12	50	31	45- 90	400	6,700
3.....	12	54	23	45- 90	500	6,300

Three shields of different manufacture were tested. All supports were two-legged, lemniscate shields of the same basic configuration; the intent was to see if shields of the same basic design exhibited similar stiffness characteristics. A description of the type of shields tested is provided in appendix A.

A physical comparison of the three shield speciments is shown in table 1. The capacities of the three shields were 360, 400, and 500 st, respectively. Since all three shields are two-legged designs, yield pressures were similar, ranging from 6,100 to 6,700 psi. Physically, shields 2 and 3 were very similar in size and weight, while shield 1 had a significantly smaller canopy and base, resulting in smaller canopy and base contact areas. Shield 1 was also designed to operate at greater heights (60 to 130 in) than shields 2 and 3 (45 to 90 in).

TEST PROCEDURE--SHIELD STIFFNESS DETERMINATIONS

The stiffness coefficients (K_1, K_2, K_3, and K_4 of equations 2 and 3) were determined from controlled displacement loading of the shield specimens in the MRS, a load simulator developed by the Bureau of Mines. A description of the MRS and its capabilities is provided in appendix B. The simulator is active in both the vertical and horizontal axes and can be programmed to operate independently in each axis, allowing a shield to be subjected to controlled vertical and horizontal displacements. All results presented in this report are based on a shield canopy and base in full contact with the load platens while the shield is restrained horizontally at the base and canopy tip.

Examination of equations 2 and 3 and figures 4 and 5 reveals how the shield stiffness coefficients were determined. By commanding the MRS to maintain a fixed horizontal displacement of the platen (fig. 4), the shield is subjected to pure vertical displacement. Terms $K_2\delta_h$ and $K_4\delta_h$ of equations 2 and 3, respectively, then become zero, since $\delta_h = 0$, leaving $F_v = K_1\delta_v$ and $F_h = K_3\delta_v$. From the

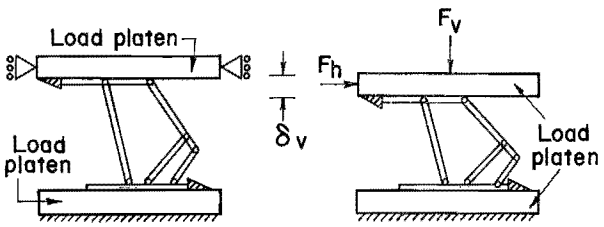

$F_v = K_1\delta_v + K_2\delta_h \rightarrow \delta_h = 0 \rightarrow F_v = K_1\delta_v$

$F_h = K_3\delta_v + K_4\delta_h \rightarrow \delta_h = 0 \rightarrow F_h = K_3\delta_v$

FIGURE 4.—Vertical shield displacement tests.

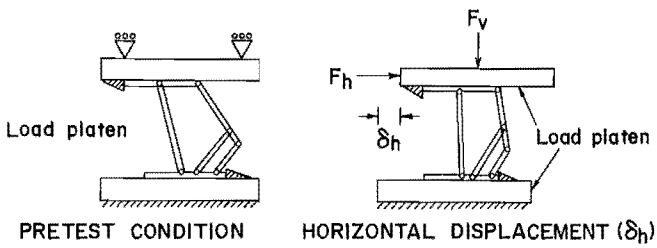

$F_v = K_1\delta_v + K_2\delta_h \rightarrow \delta_v = 0 \rightarrow F_v = K_2\delta_h$

$F_h = K_3\delta_v + K_4\delta_h \rightarrow \delta_v = 0 \rightarrow F_h = K_4\delta_h$

FIGURE 5.—Horizontal shield displacement tests.

TABLE 2. - Summary of test parameters

Shield	Operating height, in	Setting pressure, psi
1.....	78, 90, 102	≈1,000, 2,500, 3,500
2.....	57, 68, 78	≈1,000, 2,500, 3,500
3.....	58, 78	≈1,000

vertical shield displacement and associated reactive forces of the shield, stiffness parameters (K_1 and K_3) can be calculated: K_1 is equal to the ratio of the resultant vertical shield load to the vertical displacement, and K_3 is equal to the ratio of the resultant horizontal load to the vertical displacement. Likewise, subjecting the shield to pure horizontal (face-to-waste) displacement (fig. 5) permits determination of stiffness coefficients K_2 and K_4 as terms $K_1\delta_v$ and $K_3\delta_v$ of equations 2 and 3, respectively, become zero for $\delta_v = 0$.

The stiffness of a shield structure is dependent upon the initial load conditions (setting pressure), configuration (height) of the support, and other factors. Two of the three shield specimens were tested at three heights; the third shield was tested at only two heights due to limited availability of the shield. Three setting pressures were evaluated: approximately 1,000, 2,500, and 3,500 psi. A summary of the test parameters for each of the three shield specimens is documented in table 2.

The displacement load profile applied through full canopy and base contact to the shield specimens is illustrated in figure 6. The shield was set at the desired shield height with the designated setting pressure. After being set, the shield was displaced vertically until the leg pressure approached the yield pressure with no horizontal displacement the canopy relative to the base (fig. 4). Upon completion of vertical displacement, the canopy was displaced horizontally relative to the base (fig. 5) to a maximum of 350 kips of horizontal load or until the shield became unstable.

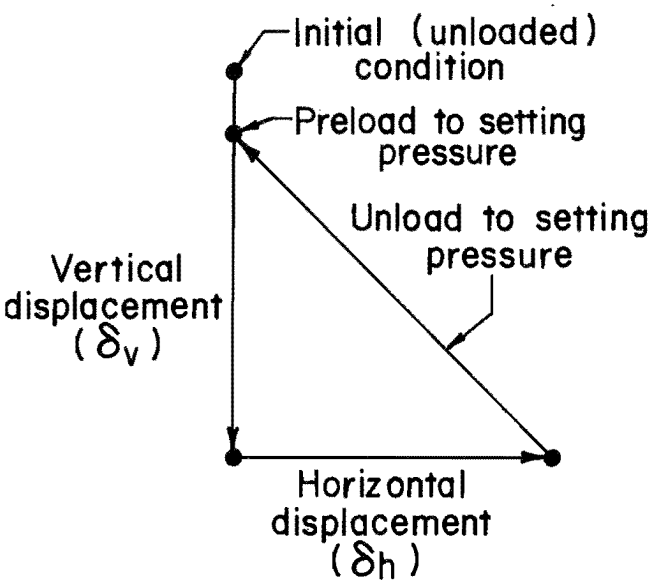

FIGURE 6.—Displacement load profile.

TEST RESULTS--SHIELD STIFFNESS CHARACTERISTICS

The test results are presented in terms of the stiffness coefficients (K_1, K_2, K_3, and K_4) associated with the elastic stiffness model as described in equations 2 and 3. Shield stiffness characteristics are discussed for each of the three shield specimens as a function of shield height and setting pressure.

SHIELD HEIGHT

The effects of shield height on shield stiffness are illustrated in figures 7 and 8. Each of the three shield specimens exhibited a decrease in stiffness with increases in shield height, meaning the supports provided less resistance at higher heights for the same change in displacement. The relationship of the stiffness response of the shields to changes in shield height was fairly linear. Shield 2 exhibited an apparent anomalous behavior at 2,500 psi setting pressure: the shield stiffness, particularly coefficient K_3, exhibited more of a quadratic relationship to

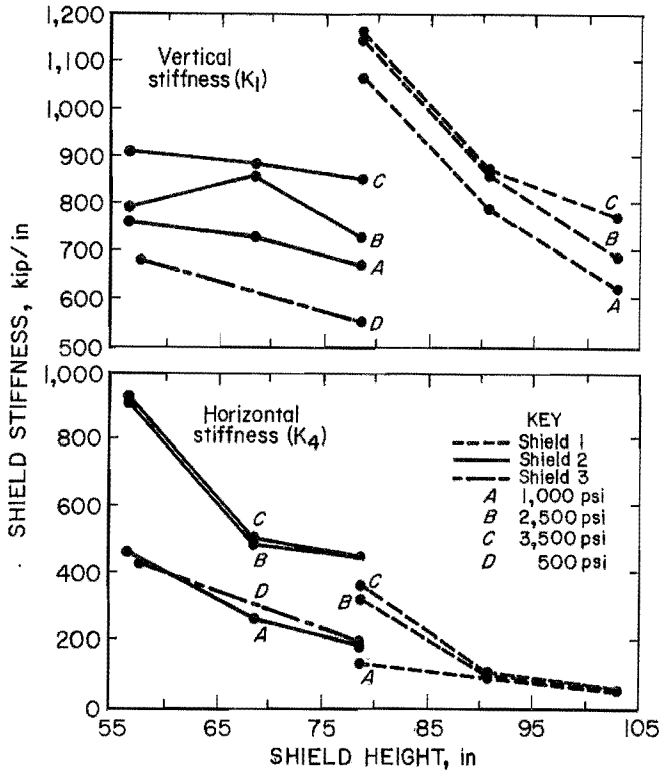

FIGURE 7.—Vertical and horizontal shield stiffness as a function of shield height.

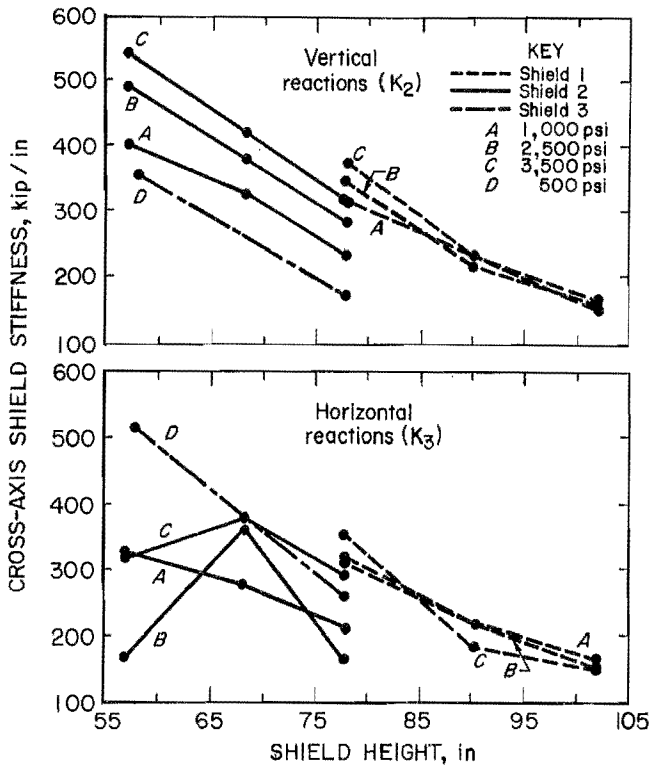

FIGURE 8.—Cross-axis shield stiffness as a function of shield height.

shield height. The cause of this anomalous behavior is unknown. The overall trend was a linear relationship between shield stiffness and shield height.

Vertical Shield Stiffness

The vertical stiffness (K_1) of the shields is illustrated in figure 7. The stiffness values were not consistent among all three shields throughout the range of heights investigated. Specifically, shield 1 was somewhat stiffer than would be expected if the results of the other two shields were extrapolated to higher heights. It should be noted, however, that the operating range of shield 1 was significantly higher than the other two shields. While shield 1 was stiffest vertically, it was also the most sensitive to changes in shield height, as illustrated by the slopes of the stiffness curves in figure 7. Hence, for shield 1, the support resistance and interaction with the strata will be significantly different when the shield is operated at different heights.

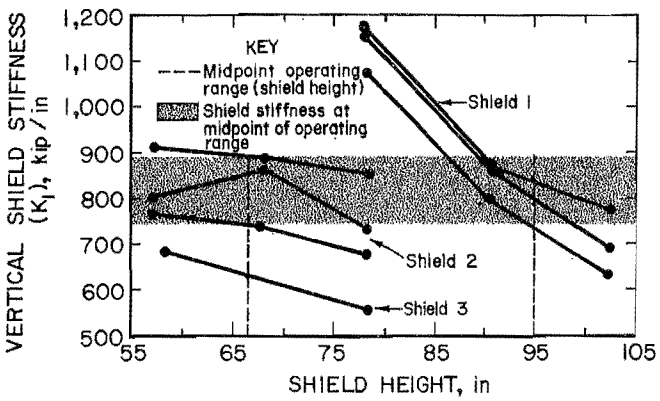

FIGURE 9.—Vertical stiffness characteristics at midpoints of operating range.

Comparing stiffness values at the midpoints of their respective operating ranges, shields 1 and 2 exhibited similar vertical stiffnesses (fig. 9), while shield 3 was significantly lower. Therefore, at the midpoints of their operating ranges, shields 1 and 2 will provide similar support resistance, while shield 3 will provide substantially less support resistance for the same change in vertical (roof-to-floor) strata convergence.

In summary, all shields exhibited a reduction in vertical stiffness as shield height was increased. The relationship between stiffness and shield height is fairly linear for individual shields. A universal vertical stiffness coefficient for all three shields is not apparent from the data, but a general trend of decreasing stiffness with increasing height for shields of the same basic configuration (i.e., two-legged lemniscate shields) seems likely.

From examination of shield components and their kinematics, it can be ascertained that vertical shield stiffness is most influenced by the stiffness of the leg cylinders. As the shield height increases, the legs are extended and become less stiff. The cylinder walls balloon under pressure, and as the legs are extended, the cylinder volume increases, making the legs more flexible. Conversely, as the shield height is reduced, the legs collapse and become axially stiffer. Under full canopy and base contact conditions, the stiffnesses of the canopy and base have little influence on overall shield stiffness, since deformation (bending) of the canopy and base is minimized.

Horizontal Shield Stiffness

Horizontal shield stiffnesses (K_4) are illustrated in figure 7. Horizontal stiffness describes horizontal shield reactions to horizontal displacements. All three shields were found to be less stiff horizontally than vertically ($K_4 < K_1$). The largest difference in horizontal and vertical stiffness occurred for shield 1, which was also the most flexible (least stiff) of the three shields horizontally and the most stiff vertically.

Horizontal shield stiffness is largely dependent upon the geometric orientation of the caving shield, lemniscate links, and legs. For shields of the same basic dimensions, these components are oriented more in the vertical axis as the shield height increases. For shield 1, which was operated at higher heights, horizontal flexibility (low stiffness) was observed, as expected. If the results of shields 2 and 3 were extrapolated to higher heights, these shields would exhibit horizontal stiffnesses similar in magnitude to that of shield 1. Hence, the horizontal capacity of a shield is reduced as the operating height of the shield increases.

In summary, shields can accommodate larger displacements horizontally than vertically, since higher reaction forces are produced vertically than horizontally for equal vertical and horizontal displacements. Shields operated at low heights will provide more horizontal resistance than shields operated at higher heights when subjected to the same horizontal displacements.

Cross-Axis Shield Stiffness

The cross-axis stiffness coefficients (K_2 and K_3), which describe vertical force shield reactions produced by horizontal displacements and horizontal force reactions produced by vertical displacements, respectively, are illustrated in figure 8. The same linear relationship, with a decrease in stiffness associated with increasing shield heights, was found for the K_2 and K_3 coefficients as was found for the K_1 and K_4 coefficients. The stiffness associated with horizontal displacements (K_2) is more consistent among all three shields throughout the height range investigated than shield stiffness associated with vertical displacements (K_3).

The principle of superposition is suggested because of the linear stiffness responses and elastic behavior of the shields, which is demonstrated in the similar magnitudes of K_2 and K_3 for individual shields. If superposition can be verified in future tests under various contact loading conditions, this would permit more complex contact conditions to be analyzed as an accumulation of simpler ones and the use of energy principles to derive displacements (Castigliano's 2nd theorem).[5]

Comparing vertical force produced by vertical displacements (K_1) and vertical

[5]Pages 407-408 of work cited in footnote 4.

force produced by horizontal displacements (K_2), approximately 2 to 3 times more vertical force was produced from vertical displacements than was produced from horizontal displacements. This was due to leg orientation and horizontal shield stiffness contributed by the caving shield-lemniscate components. Face-to-waste displacement of the canopy tends to rotate the leg cylinder towards a more vertical position, which produces a vertical support reaction. However, this motion is constrained by the caving shield-lemniscate system, which helps prevent face-to-waste displacement of the canopy.

The significance of the K_2 stiffness coefficient should be recognized. Significant vertical forces are developed from horizontal displacements. Since horizontal displacements produce a vertical support reaction without any vertical roof convergence (assuming no further compaction of the roof), the capacity of the support to resist vertical (roof-to-floor) convergence is reduced by the amount of vertical force produced by horizontal displacements. Since the primary function of the support is to resist vertical roof convergence, this cross-axis interaction is undesirable. Ideally, a vertical displacement should produce only a vertical support reaction, and a horizontal displacement should produce only a horizontal reaction.

A similar analysis can be applied to K_3 (horizontal force produced by vertical displacements). Considerably more horizontal force is produced by horizontal displacements than by vertical displacements, but the horizontal force produced by vertical displacements is significant and should be considered in an analysis of support behavior.

SETTING PRESSURE

The effect of setting pressure on shield stiffness is illustrated in figures 10 and 11. The effect of setting pressure on shield stiffness was not as significant as the effect of shield height.

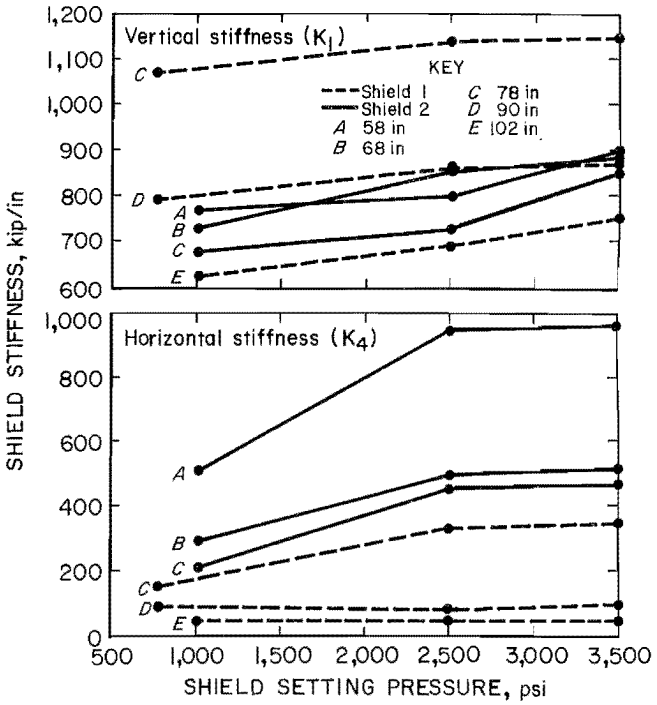

FIGURE 10.—Effect of setting pressure on vertical and horizontal shield stiffness.

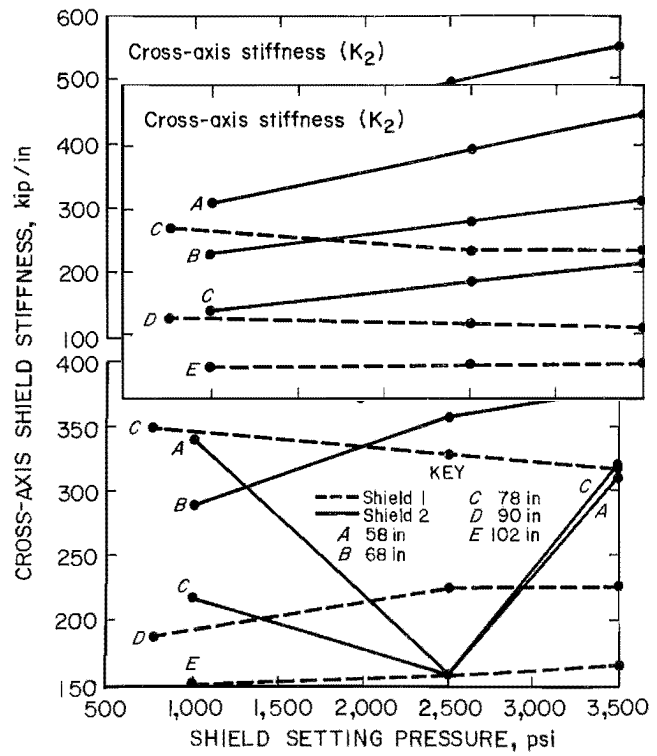

FIGURE 11.—Setting pressure effects on cross-axis stiffness coefficients.

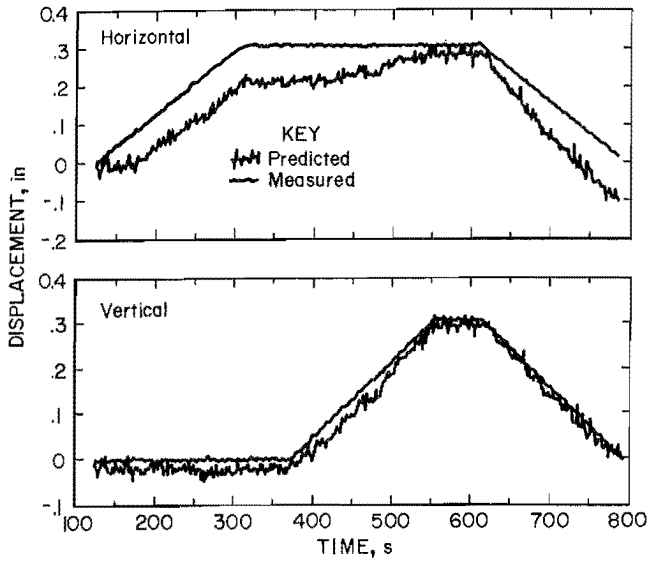

FIGURE 12.—Predicted shield displacements from leg orientations and leg pressure measurements.

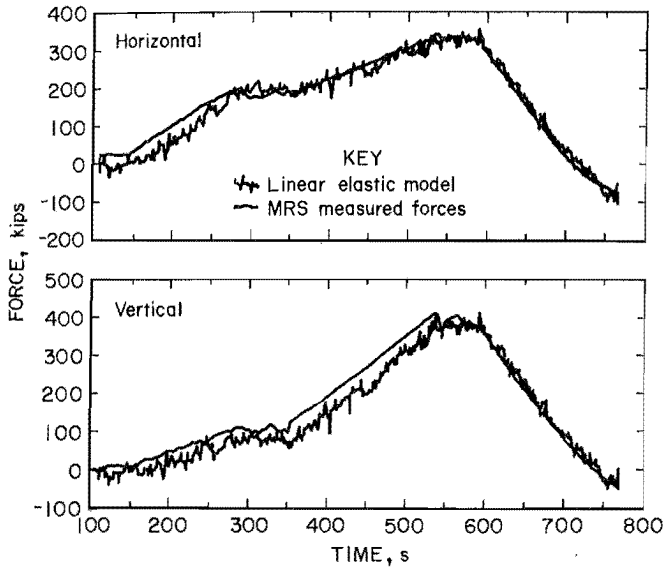

FIGURE 13.—Force predictions from shield stiffnesses.

Shield 2 showed a slight increase in stiffness with increases in pressure, while for shield 1, changes in setting pressure produced almost no change in stiffness. Shield 3 was evaluated at only one setting pressure, due to limited shield availability. The data also indicate that the effect of setting pressure was largely independent of changes in shield geometry due to changes in height, as the slopes (profile) of the setting pressure curves in figures 12 and 13 are very similar. A significant change in shield stiffness was noted for shield 2 at low setting pressures (below 2,500 psi), but above 2,500 psi, setting pressure had little effect on horizontal stiffness.

Since a change in setting pressure relates primarily to the compressibility of the hydraulic fluid in the leg cylinder, it is unlikely that the leg stiffness would be altered sufficiently to produce a change in overall shield stiffness. A small change in setting pressure (e.g. from 2,500 psi to 3,000 psi) has almost no effect on shield stiffness. Hence, it is concluded that shield stiffness is independent of setting pressure for the range of setting pressures likely to be encountered underground (2,500 to 3,500 psi).

SHIELD LOAD PREDICTIONS FROM SHIELD STIFFNESSES

Once the stiffness characteristics of the shield(s) are determined, vertical and horizontal force reactions can be determined from equations 2 and 3 if shield displacements are known. Tests in the MRS showed that shield displacements could be determined effectively by measurement and analysis of a change in leg angle relative to the plane of the canopy and a change in leg pressure (or leg compression), as illustrated in figure 12. Using the displacement predictions from figure 12 as input to the elastic stiffness model (equations 2 and 3), the vertical and horizontal force predictions illustrated in figure 13 were determined. The resulting force predictions are quite good considering the errors in displacement inputs.

CONCLUSIONS

An investigation of the stiffness characteristics is a first step in an elastic analysis of shield structures. From this initial study, a basic understanding of the load-displacement relationship of a shield structure has been determined. The basic research conducted in this study provides a foundation upon which stress optimization and support-strata interaction studies can be made to improve longwall support design and utilization. Conclusions drawn from this research are summarized as follows:

1. The load-displacement relationship of shield supports can be effectively modeled by an elastic stiffness model with two degrees of freedom.

2. Three shields of different manufacture, but of the same basic design (two-legged, lemniscate shields), exhibited similar stiffness characteristics.

3. Changes in shield height have a significant effect on shield stiffness; increasing shield height resulted in reduced shield stiffness. The relationship between shield stiffness and height showed a linear tendency, but additional data are required to provide conclusive evidence of this behavior.

4. Higher reactive forces will occur at lower shield heights, indicating a reduction in support resistance (for equal displacements) when shield operating heights are increased.

5. Shields are generally stiffer vertically than horizontally, indicating that they will react greater loads to vertical (roof-to-floor) convergence than horizontal (face-to-waste) displacements of the same magnitude.

6. Shield stiffness is relatively insensitive to changes in setting pressure, particularly when setting pressures exceed 2,500 psi.

7. The elastic behavior of the shield suggests that the principle of superposition may be applicable to determine complicated load conditions from simpler ones.

APPENDIX A.--DESCRIPTION OF SHIELD SUPPORTS

The shield specimens used in these tests were all of the same basic configuration, classified as a two-legged, lemniscate shield. This shield design is characterized by two leg cylinders, which act between the base and canopy components to resist strata convergence. A canopy capsule cylinder acts between the canopy and caving shield to provide stability and control the atitude of the canopy. The caving shield and lemniscate links connect the canopy to the base and provide resistance to horizontal loading. The major components of the shield are illustrated in figure A-1.

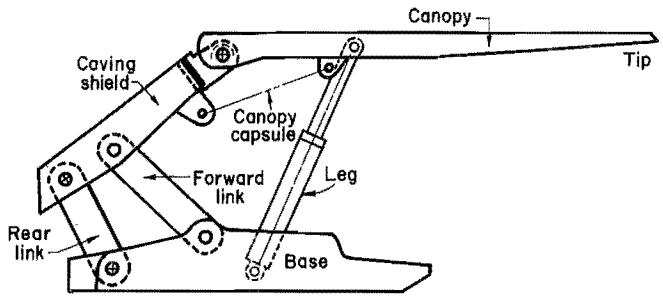

FIGURE A-1.—Shield support.

APPENDIX B.--DESCRIPTION OF MINE ROOF SIMULATOR

The Mine Roof Simulator (MRS) is a large hydraulic press (fig. B-1) designed to simulate the loading of full-scale underground mine roof supports. The MRS is unique in its abilities to apply both a vertical and a horizontal load simultaneously.

Both the vertical and horizontal axis can be programmed for either force or displacement control. This capability permits tests, such as true friction-free controlled loading of shields, that cannot be accomplished in uniaxial test machines since the shield reacts a horizontal load to vertical roof convergence. Friction-free tests of this nature can be accomplished in the MRS by allowing the platen to float in the horizontal axis by commanding a zero horizontal load condition. Likewise, the MRS can apply controlled horizontal loading to a shield support, whereas, uniaxial test machines can only apply vertical loading, with no control over horizontal load reactions or capability to provide a specified horizontal load to the structure. The controlled displacement capability of the MRS allows determination of a structure's stiffness, which is essential to understanding the load-displacement characteristics of the structure.

The machine incorporates 20-ft square platens with a 16-ft vertical opening, enabling full-scale testing of longwall support structures. Its capacity is 1,500 st of vertical force and 800 st of of horizontal force. Controlled displacement ranges 24 in vertically and 16 in horizontally. Load and displacement control is provided in four ranges operating under a 12-bit analog-to-digital closed-loop control network, providing a load control capability of better than 0.1 kips (100 lb) and displacement control capability of better than 0.001 in. in the smallest load-displacement range.

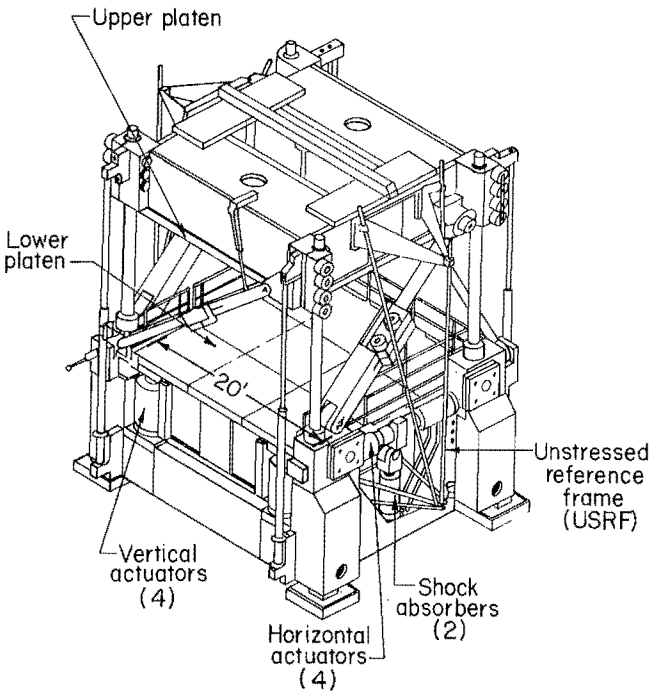

FIGURE B-1.—Mine Roof Simulator.

MRS control and data acquisition is achieved by a computer. Eighty-eight channels of test specimen transducer conditioning are provided. Data acquisition is interfaced with the control network so that behavior of the MRS can be controlled by response of the test article, as indicated by instrumentation. For example, tests can be terminated or held when strain values reach a designated level in specified areas of the support structure. High-speed data acquisition is available with a separate computer at a rate of 300 samples per second. An X-Y-Y recorder provides real-time plotting of three data channels. All data are stored on computer disks for subsequent processing and analysis.

APPENDIX C.--NOMENCLATURE

K_1 - Vertical shield stiffness coefficient. Ratio of vertical force to vertical shield displacement.

K_2 - Cross-axis shield stiffness coefficient. Ratio of vertical force to horizontal shield displacement.

K_3 - Cross-axis shield stiffness coefficient. Ratio of horizontal force to vertical displacement.

K_4 - Horizontal shield stiffness coefficient. Ratio of horizontal force to horizontal displacement.

Horizontal displacement - Face-to-waste strata movement resulting in displacement of canopy relative to the base.

Vertical displacement - Roof-to-floor strata convergence.

INT.-BU.OF MINES,PGH.,PA. 28642

U.S. GOVERNMENT PRINTING OFFICE: 1988 — 605-017/80,002